

Conditional data processing for single-shot spectral analysis by use of laser-induced breakdown spectroscopy

Jorge E. Carranza, Kenjiro Iida, and David W. Hahn

Schemes of conditional data processing are evaluated based on either the peak-to-base ratio or the signal-to-noise ratio as a metric for analyte detection in single-shot laser-induced breakdown spectra. The analyte signal investigated is the 288.1-nm Si I emission line provided by an aerosol stream of monodisperse 2.5- μm -sized silica microspheres. Both the Si emission line and a spectral region corresponding to continuum emission are used to evaluate the statistical distribution of spectral noise. The probability of false hits is determined by evaluating various conditional processing thresholds. As the detection threshold increases, the rate of detected silica particle hits decreases along with the expected fraction of false-particle hits (i.e., spectral noise). For all threshold values the signal-to-noise ratio is found to provide a more robust metric for single-shot analyte detection compared with the peak-to-base ratio. © 2003 Optical Society of America

OCIS codes: 140.3440, 300.0300, 300.6210.

1. Introduction

The analysis of ambient air aerosols has been the concern of the scientific community in recent years because of their potential adverse effects on human health, visibility, and climate changes.^{1–3} In response to these analysis needs, analytical techniques such as laser-induced breakdown spectroscopy (LIBS) can be applied to providing particulate matter data that can assist in understanding the dynamics of these pollutants. Researchers have successfully applied LIBS in a number of studies involving aerosol particles, including effluent waste streams and real-time monitoring.^{4–11} A novel feature of LIBS for aerosol analysis is the ability to provide elemental mass composition and size data of individual particles.¹² LIBS for particle sizing takes advantage of the inherent point-sampling quality of the technique in combination with the discrete nature of aerosols to make possible identification of single-shot LIBS spectra corresponding to individual aerosol particles.

The use of conditional analysis, however, requires a suitable scheme for identifying these single-shot spectra, which necessitates consideration of issues such as the spectral noise characteristics and subsequent rejection of false particle hits. Spectral data processing as applied to LIBS-based conditional analysis is the subject of this paper.

2. Conditional Data Analysis

In earlier publications Hahn and co-workers developed a conditional analysis scheme for single-particle detection.^{12,13} As typically applied, each LIBS spectrum is analyzed by using the emission intensity about the expected analyte peak compared with the emission intensity of an adjacent, featureless continuum spectral region. A spectrum is classified as representative of a particle hit if the ratio of the emission intensities (peak to continuum) exceeds a threshold value, which is typically set to provide between 0.1% and 0.5% false hits. A false hit is defined as a spectrum that exceeds the threshold but contains no targeted analyte in the corresponding plasma volume. To avoid eliminating the detection of actual but weak analyte signals that are comparable with the larger noise fluctuations, it is desirable to set the threshold so that some false hits are recorded, hence the 0.1–0.5% false-hit rate. The discrimination between legitimate analyte signals (i.e., true hits) and spectral noise spikes (i.e., false hits) may be addressed with an

The authors are with the Department of Mechanical and Aerospace Engineering, University of Florida, Gainesville, Florida 32611. The e-mail address for D. W. Hahn is dwhahn@ufl.edu.

Received 10 February 2003; revised manuscript received 16 June 2003.

0003-6935/03/306022-07\$15.00/0

© 2003 Optical Society of America

additional postprocessing scheme in which the multiple emission lines of the targeted analyte are used. This is based on the premise that extreme noise fluctuations sufficient to trigger a false hit are statistically unlikely to be present on multiple analyte lines. This approach has proved successful in the earlier studies cited above; however, multiple atomic emission lines in a given spectral window are not always available. It is therefore useful to explore schemes that make use of a single atomic emission line corresponding to the targeted analyte species. In the present paper, two data-processing schemes are explored and compared in the context of LIBS-based particle detection and single-shot spectral analysis.

3. Experimental Methods

A brief overview of the LIBS experimental setup is presented here with additional details reported previously.¹⁴ The excitation source was a 1064-nm Q-switched Nd:YAG laser with a nominal pulse width of 10 ns and pulse energy of 290 mJ and operated with a 5-Hz pulse repetition rate. The laser pulse-to-pulse energy stability was $\pm 4\%$ rms. The expanded laser beam (12-mm diameter) was focused into the particle source stream with a 75-mm UV grade plano-convex lens to create the plasma. The plasma emission was collected along the incident beam in a backward direction (180°) and separated with a pierced mirror. The collected plasma emission was fiber coupled to a 0.275-m spectrometer, dispersed with a 2400-groove/mm grating (0.03 nm/pixel, 0.12-nm resolution), and recorded with an intensified CCD array detector.

A significant motivation for the present study is investigation of the role of aerosol particles in combustion system emissions; hence the particle source stream was the exhaust gas stream of a laboratory scale hydrogen-air burner seeded with aerosol particles. The gas stream was confined within a 6.4 cm \times 6.4 cm stainless-steel chimney with optical access provided by UV grade quartz plates mounted along opposing sides. The chimney was nominally 1 m in length, and the gas temperature at the LIBS sample point was in the range of 650 K. Aerosols were generated by nebulizing a 2.5- μm monodisperse silica (SiO_2) particle suspension and by passing the resulting aerosol stream into the combustion system. The nebulized particle suspension concentrations were adjusted to produce a final aerosol concentration at the LIBS sample point of ~ 60 or 120 particles/ cm^3 . The uncertainty of the particle concentration is estimated to be $\sim 20\%$ based on previous experience, including light-scattering measurements, with the current aerosol systems.

4. Methodology and Results

In the present paper, two different approaches are compared for single-shot spectral conditional analysis with the goal of individual particle detection. The processing schemes are based on two different metrics used to identify single-shot spectra containing the targeted analyte emission, namely, the peak-

to-base (P/B) ratio and the signal-to-noise ratio (SNR). For the present analysis the SNR is defined as the ratio of the integrated atomic emission line intensity (peak area) to the average noise of the adjacent, featureless continuum intensity (i.e., rms noise). The rms was determined from the deviation of a least-squares fit over a narrow spectral region corresponding to ~ 40 pixels. Similarly, the P/B ratio is defined as the ratio of the integrated atomic emission line intensity (peak area) to the average intensity of the adjacent, featureless continuum emission (i.e., plasma baseline). The analyte peak line used for all analyses is the Si I atomic emission line at 288.1 nm. As discussed above the goal of the present analysis is to categorize efficiently and accurately each collected spectrum as either containing the targeted analyte signal (i.e., a particle hit) or missing the targeted analyte signal (i.e., a particle miss).

For the present study, two sets of spectral data were collected and stored for analysis, which will be referred to as set A and set B. Spectral set A corresponds to the collection of 57,511 individual laser shots recorded at a nominal silica microsphere concentration of 120 particles/ cm^3 . Spectral set B corresponds to the collection of 28,889 single laser shots recorded at a nominal silica microsphere concentration of 60 particles/ cm^3 . All spectra were then analyzed by conditional analysis schemes based on either the SNR or the P/B ratio with the goal of detecting spectra corresponding to the presence of a silica microsphere, as based on the Si 288.1-nm emission line.

The fundamental task in conditional data analysis is selection of the appropriate threshold value for the P/B ratio or for the SNR to quantify a given spectra as corresponding to a particle hit or particle miss. Throughout the remainder of this paper the designation of a spectrum as a hit refers to the Si 288.1-nm atomic emission signal (either the SNR or P/B ratio) exceeding the predetermined threshold value. Conversely, a spectrum in which the spectral region of the Si 288.1-nm atomic emission does not exceed the threshold value is designed as a miss. In addition to the calculated P/B ratio and SNR corresponding to the Si atomic emission line, the P/B ratio and SNR values were calculated corresponding to a featureless continuum region (0.15-nm band centered at ~ 289.5 nm) of similar baseline intensity adjacent to the Si emission line. For comparison and discussion the P/B rates and the SNR values of the 288.1-nm Si emission line are referred to as the Si peak or on-peak values, whereas the P/B ratio and the SNR values of the adjacent continuum region are referred to as the off-peak values. The off-peak values are taken as representative of the on-peak values with respect to spectral noise fluctuations (i.e., white spectral noise). Therefore the off-peak values enable selection of the appropriate conditional analysis threshold values without collecting an additional set of spectral data in the absence of the targeted analyte species.

Additional comments are offered with respect to

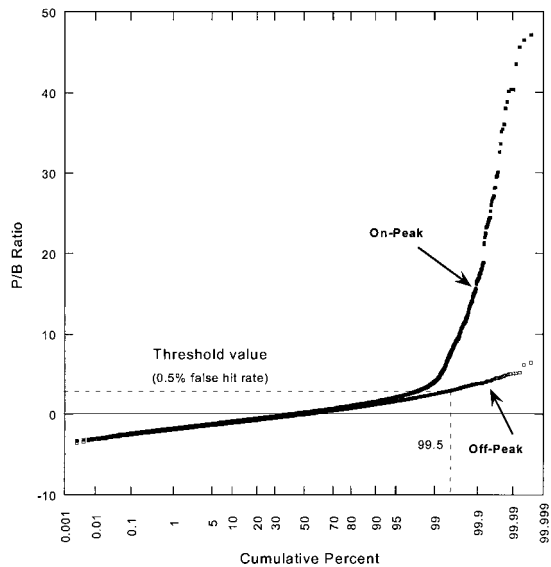


Fig. 1. Cumulative distribution of the P/B ratio for the 288.1-nm silicon emission line (on peak) and the adjacent continuum region (off peak) for data set A. The threshold value corresponds to a 0.5% false-hit rate.

selection of the continuum region and the off-peak spectral locations. We also ran analyses by using an alternative off-peak spectral location shifted from 289.5 to 290.0 nm (i.e., a shift of 16 pixels) and, to calculate the rms spectral noise, by using a similarly shifted continuum region. These alternative analyses yielded essentially the same results as presented below. Although a detailed parametric study of the continuum region selection was not included in this work, two points are noted. The continuum region should be selected to reflect comparable noise and intensity as the analyte peak, while being free of any interfering atomic emission lines; however, the precise spectral location within these guidelines is not considered critical.

For the case of the P/B approach the threshold value is typically set to produce between 0.1% and 0.5% false-hit rates (i.e., off-peak hits or hits with no analyte present), as reported previously.^{12,13} For the present analysis an initial false-hit rate of 0.5% was utilized. In addition a substantially reduced false-hit rate of 0.05% was investigated. For both spectral data sets, A and B, the threshold was determined by calculating the P/B ratio corresponding to the off-peak region of each spectra and then defining the threshold P/B value so that exactly 0.5% or 0.05% of the total spectra exceeded the value. The calculated 0.5% P/B threshold values were 2.86 and 2.78 for spectral data sets A and B, respectively. A graphic representation of this process is shown in Fig. 1, where cumulative distributions of the on-peak and off-peak P/B ratio for all spectra of data set A are plotted. Figure 1 shows that the P/B ratio corresponding to the off-peak region, which characterizes the level of shot-to-shot spectral noise, follows a normal distribution, in that ~50% of the shots are char-

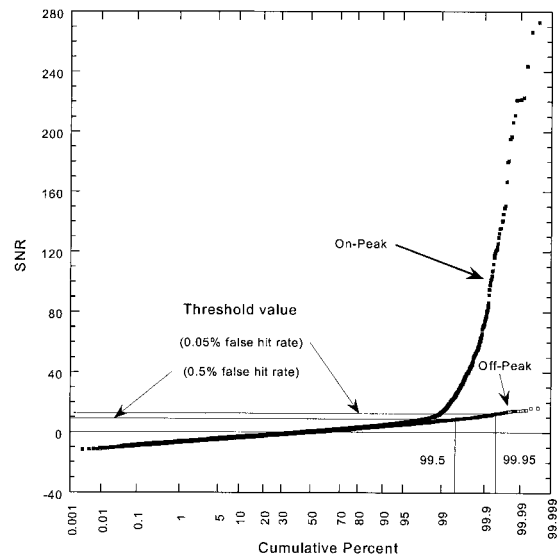


Fig. 2. Cumulative distribution of the SNR for the 288.1-nm silicon emission line (on peak) and the adjacent continuum region (off peak) for data set A. The threshold values correspond to 0.05% and 0.5% false-hit rates.

acterized by a P/B value either below or above zero. Nearly identical noise behavior is noted for the on-peak P/B values given the overlap of the distribution functions until the threshold value is approached. The rapid departure of the two P/B distribution functions at the conditional analysis threshold value is attributed to the enhanced P/B ratios on the silica atomic emission line because of the presence of actual silica particle hits.

Note that the on-peak Si P/B values above the threshold greatly exceed even the largest P/B values of the off-peak values, which are considered the extreme spectral noise fluctuations. The above results support the conclusion that the spectral noise fluctuations are characterized by white noise over moderate spectral regions and that the use of a suitable (i.e., comparable intensity) off-peak region for selection of the conditional analysis threshold is justified.

For the case of the signal-to-noise approach the threshold values were determined similarly to the process explained above as based on the SNR. The threshold limits were determined for an off-peak false-hit rate of 0.05% in addition to the false-hit rate of 0.5%. Figure 2 shows the cumulative distribution of all the shots for the spectral data set, A. Both data sets, A and B, revealed essentially identical cumulative distributions of the off-peak noise, including a 50% value near a SNR ratio of zero. However, the on-peak distribution for set A was observed to break from the off-peak value earlier than the on-peak distribution of set B, as observed in Fig. 3, which presents both data sets with a reduced SNR axis to highlight this behavior. The cumulative distribution of set A reflects the higher silica particle concentration corresponding to set A (~120 particles/cm³) compared with set B (~60 particles/cm³); hence a

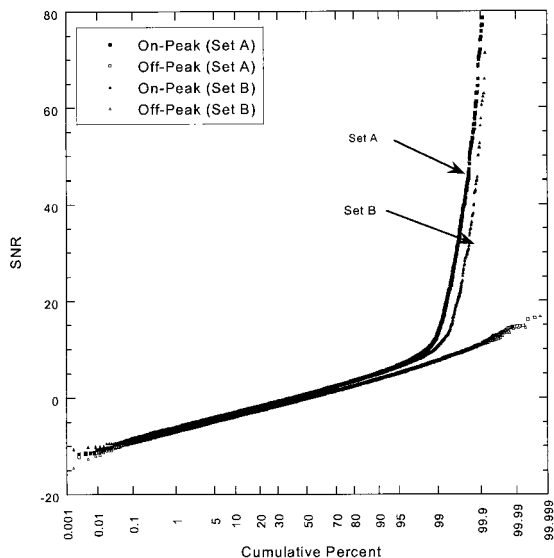


Fig. 3. Cumulative distribution of the SNR for the 288.1-nm silicon emission line (on peak) and the adjacent continuum region (off peak) for both data sets, A and B. The y axis has been expanded to emphasize the smaller SNR values.

higher percentage of particle hits is expected. Based on Poisson statistics the particle-hit rate should scale linearly with the particle concentration for low sample rates. However, a recent investigation of sampling rates revealed some departure from the ideal Poisson statistics at comparable particle concentrations.¹⁵ In addition to these comments, note that the cumulative distribution of the off-peak values are indistinguishable for the two data sets, as expected. The SNR threshold values corresponding to the 0.5% false-hit rate was calculated as 8.66 for the Fig. 2 data. Based on the more stringent definition of off-peak false hits, the SNR threshold value for the 0.05% false-hit rate was calculated to the 12.4. Comparison of the two threshold values reveals only a small change in the cumulative distribution of the on-peak SNR values at the threshold point (98.9% at the 0.05% threshold and 97.7% at the 0.5% threshold), despite the order-of-magnitude change in the off-peak false-hit rates.

To access the relative difference in identified spectral hits as calculated with the threshold values based on either the P/B ratio or SNR, all the spectral data were processed simultaneously by using both parameters and compared relative to one another. A Venn diagram of the number of spectral hits satisfying each approach is shown in Fig. 4 for the Set A data at threshold values based on either 0.05% or 0.5% false hits. The SNR approach yields a larger collection of Si particle hits than the P/B approach for each false-hit level. Specifically, for the 0.5% false-hit threshold, the collected hits total 1355 and 1251 for the SNR and P/B approach, respectively. For the 0.5% threshold it is expected that statistically these totals both reflect approximately 289 false hits based on the total number of spectra (57,511). For

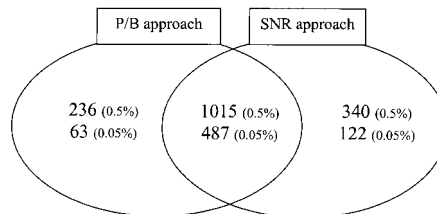


Fig. 4. Venn diagram of the conditionally analyzed particle hits when the P/B and SNR approaches are used for data set A at thresholds values corresponding to either 0.5% and 0.05% false-hit rates.

the 0.05% false-hit threshold the collected hits total 609 and 550 for the SNR and P/B approach, respectively, and are expected to each contain an average of 29 false hits (i.e., 0.05% of 57,511). As noted above a decrease in the false-hit rate by a factor of 10 produces a decrease in collected hits by a factor of only ~ 2 for each approach. As a consequence of the more restrictive threshold value, the influence of false hits on the total number of collected hits is significantly diminished (e.g., from 289/1355 or 21% to 29/609 or 4.7% for the SNR approach).

It is useful to examine the resulting spectra as identified from the above analyses. The ensemble-average spectra of the collected hits are plotted in Fig. 5 for a 0.5% false-hit rate as applied to data Set A. Five spectra are shown that correspond to the five unique subsets of the Venn diagram in Fig. 4 for the 0.5% threshold, namely, spectra that exceed both the P/B and SNR thresholds, spectra that exceed the SNR threshold, spectra that exceed the P/B thresh-

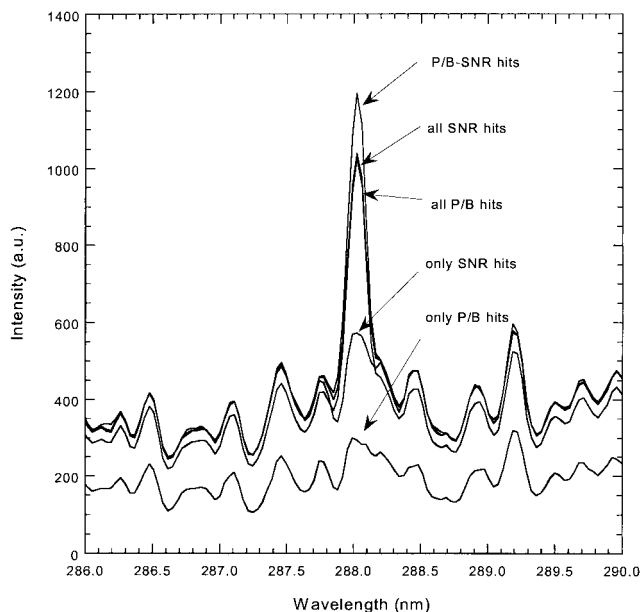


Fig. 5. Ensemble-averaged spectra of particle hits (288.1-nm Si line) processed when the P/B and SNR approaches are used at a 0.5% false-hit rate corresponding to the Venn diagram in Fig. 4. Note that the total number of spectra averaged for each spectrum is different, as listed in Fig. 4.

old, spectra that exceed only the SNR threshold, and spectra that exceed only the P/B threshold. Two important features can be drawn from the spectra presented. First, the ensemble-averaged spectra that correspond to the threshold condition for the P/B or SNR tests, or both tests simultaneously, display a well-defined silicon atomic emission peak at 288.1 nm. Second, the spectra corresponding to the ensemble average of the hits that pass only the P/B or SNR threshold exhibit a significantly reduced silicon peak. As seen in Fig. 4 the spectrum with the most diminished silicon peak corresponds to the ensemble average of the 236 hits that passed only the P/B threshold. It is concluded that this spectrum comprised a large number of false hits, namely high spectral noise in the region of the silicon emission line. Recall that statistically speaking it is expected that ~ 289 spectra corresponding to the false hits is included in the set of P/B spectra for the 0.5% threshold value. In contrast the spectrum corresponding to the ensemble average of the 340 hits that passed only the SNR threshold reveals a more substantial silicon peak than the P/B-only spectra. However, the peak is still characterized by a marked reduction in the silicon emission peak.

Although the spectra in Fig. 5 are all ensemble-averaged spectra, each spectrum corresponds to a different number of hits. However, note the similarity of the baseline structure for all five spectra, thereby revealing the inherent baseline noise in the CCD array. For the range of total hits corresponding to the Fig. 5 data (i.e., 236–1355), no significant effects are attributed to the exact number of spectra averaged, because all spectra are characterized by a sufficient number of hits to diminish (i.e., average out) the shot noise. To further illustrate the single-shot spectral noise, several individual spectra are presented in Fig. 6 along with the ensemble-averaged spectrum from Fig. 5 corresponding to the all-SNR data set. The silicon emission peaks are all comparable as expected; however, the spectral shot noise is significant, which illustrates the inherent difficulty in identifying single-shot spectra.

To investigate further the influence of the conditional analysis thresholds, we also analyzed the two data sets by varying the threshold values (as defined above by the off-peak hit rate). Figure 7 presents the resulting silicon particle sampling rate (i.e., the on-peak hit rate) for Set A as the threshold value is varied from a more restrictive 0.01% to a more relaxed value of 1% for both the P/B and SNR approaches. The resulting particle-hit rate increases monotonically with a decreasing threshold (i.e., increasing the off-peak hit rate) for both the SNR and P/B conditional sampling approaches. Also included in Fig. 7 is the calculated rate of false hits (expressed as a percentage of total hits) based on each threshold value and the corresponding total hit rate. As described above, this value corresponds to the statistically expected number of false hits divided by the total number of identified hits. As observed in Fig. 7, increasing the percentage of false hits by 1

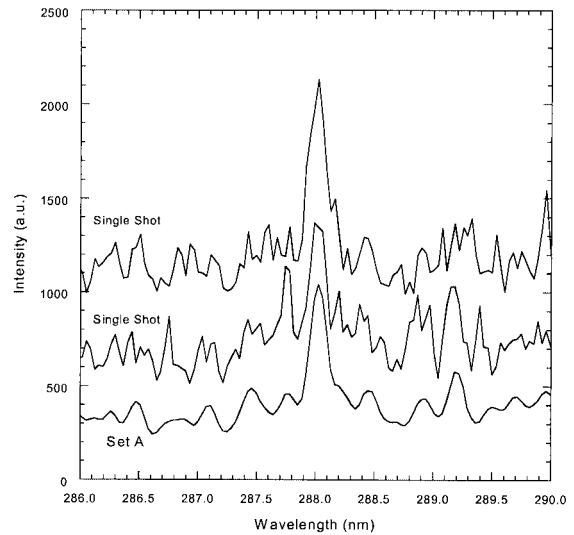


Fig. 6. Single-shot spectra of particle hits (288.1-nm Si line) as identified when the SNR approach is used along with the corresponding ensemble-averaged spectrum of the entire SNR data set corresponding to the data from the 0.5% false-hit rate of Figs. 4 and 5. All spectra have the same scale and have been shifted vertically for clarity.

order of magnitude, from 0.05% to 0.5%, increases the expected percentage of false hits from 4.7% to 21.2% for the SNR-based process and from 5.2% to 23% for the P/B-based process. In addition, note that the percentage of expected false particle hits is slightly less for all threshold cases when comparing the SNR approach with the P/B approach. This is consistent with the greater number of particle hits collected with the SNR approach compared with the P/B approach, as seen in Fig. 4, which reduces the potential influence from false particle hits.

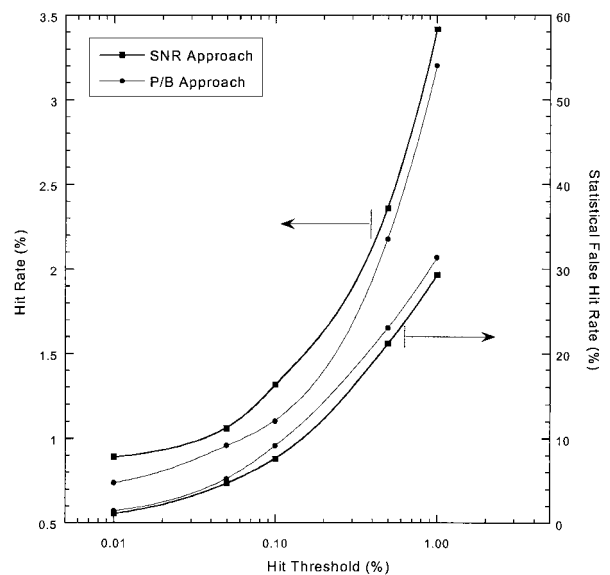


Fig. 7. Influence of the conditional processing threshold on the silica-particle-hit rate (on peak) and the corresponding expected false-hit rate (as a percentage of total hits) for data set A.

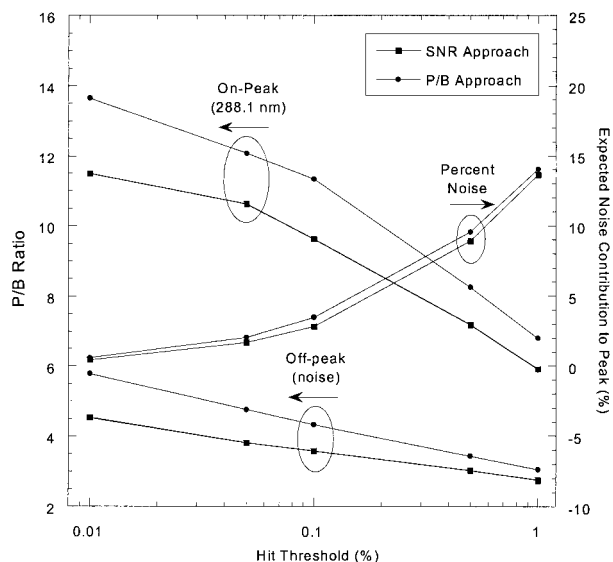


Fig. 8. Influence of the conditional processing threshold on the average P/B intensity of the silica emission line (on peak) for identified hits along with the corresponding P/B intensity of the expected noise and the expected noise as a weighted percentage of the on-peak signal.

Although the above results enable an estimate of the expected percentage of false hits for a given threshold, it remains difficult to quantify the exact contribution of such false hits to the analyte peak (288.1-nm Si line) in the resulting ensemble-averaged spectrum of all hits. For a given threshold, however, the expected contribution of false hits to the on-peak signal can be assessed by applying the same threshold to the off-peak region and calculating an ensemble-averaged spectrum based on the off-peak false hits. The resulting P/B ratio of the off-peak signal provides a quantitative estimate of the statistical noise contained in the on-peak analyte signal. Figure 8 shows the average P/B intensity of the on-peak silicon emission line and the corresponding average P/B of the off-peak noise as a function of threshold for both the SNR and P/B processing schemes. Note that for comparison purposes the P/B values of the on-peak and off-peak spectra must be weighted by the corresponding number of hits. As seen in Fig. 8 the average silicon emission line P/B signal (on peak) corresponding to the P/B approach is greater than the P/B ratio as processed with the SNR approach for all threshold values. However, the corresponding average P/B ratio of the false hits (off peak) is also greater with the P/B approach compared with the SNR approach. The fraction of the on-peak silicon signal attributed to the expected noise (the ratio of weighted off-peak to on-peak P/B signals) is also plotted in Fig. 8. The contribution of noise to the on-peak signal is minimized as the threshold value is increased (i.e., the decreasing percentage of false hits). An examination of Fig. 8 reveals a breakpoint in the noise contribution at a hit threshold value around 0.05–0.1%, with the SNR-

based noise contribution slightly less than the P/B-based values. Specifically the expected contribution of noise to the analyte peak is $\sim 2.8\%$ at a hit threshold of 0.1% and is decreased to 1.7% at a threshold of 0.05%. Both schemes produce remarkably similar results, although it is concluded that the SNR is a slightly better determinant for conditional spectral processing compared with the P/B ratio.

5. Conclusions

A conditional analysis of the single-shot LIBS spectra has been evaluated by using two approaches for detection of the targeted analyte peak, namely, the signal-to-noise ratio and the peak-to-base ratio. The key requirement for either approach is the selection of an appropriate threshold value so that spectral shot-noise fluctuations (i.e., false hits) are minimized while sufficient sensitivity to the actual analyte signal is maintained. By investigation of the number of identified analyte hits in combination with a surrogate off-peak spectral region insight was gained into the influence of the threshold value. In general the SNR parameter provides a modest increase in the spectral discrimination for single-shot processing compared with the P/B ratio. For both parameters, setting the threshold value so that the false-hit rate is between 0.05% and 0.1% provides an optimal degree of spectral discrimination between noise and actual analyte signals. The false-hit rate may be set in the presence of the targeted analyte by using an adjacent spectral region of similar intensity characterized by only continuum emission, or it may be set directly on the analyte spectral line in the absence of the targeted analyte.

Finally, note that single-shot detection of a targeted analyte species by using only a single analyte line, as addressed in this study, requires careful consideration of the detection threshold for suppression of spectral noise to be achieved while sensitivity to the analyte signal is maintained. Although the threshold may be optimized, clearly the identified set of analyte hits will always contain a number of false hits. It is recommended that additional processing be performed to further sort the identified hits. Earlier approaches that have been successfully applied include the analysis of additional analyte lines or quantitative analysis of the line profile of each analyte peak.^{12,16}

This work was supported in part by the U.S. Navy Office of Naval Research through contract N00014-0210838.

References

1. U.S. Environmental Protection Agency, Revised Standards for Hazardous Waste Combustors, Federal Register **61**(77) 17,357–17,358 (1996).
2. U.S. National Research Council, *Research Priorities for Airborne Particulate Matter: II. Evaluating Research Progress and Updating the Portfolio* (National Academies Press, Washington, D.C., 1999).
3. J. H. Seinfeld, and S. N. Pandis, *Atmospheric Chemistry and*

Physics: From Air Pollution to Climate Change (Wiley, New York, 1998).

4. D. K. Ottesen, J. C. F. Wang, and L. J. Radziemski, "Real-time laser spark spectroscopy of particulates in combustion environments," *Appl. Spectrosc.* **43**, 967–976 (1989).
5. K. C. Ng, N. L. Ayala, J. B. Simeonsson, and J. D. Winefordner, "Laser-induced plasma atomic emission-spectrometry in liquid aerosols," *Anal. Chim. Acta* **269**, 123–128 (1992).
6. S. Yalcin, D. R. Crosley, G. P. Smith, and G. W. Faris, "Spectroscopic characterization of laser-produced plasmas for *in situ* toxic metal monitoring," *Hazard. Waste Hazard. Mater.* **13**, 51–61 (1996).
7. M. H. Nunez, P. Cavalli, G. Petrucci, and N. Omenetto, "Analysis of sulfuric acid aerosols by laser-induced breakdown spectroscopy and laser-induced photofragmentation," *Appl. Spectrosc.* **54**, 1805–1816 (2000).
8. R. E. Neuhauser, U. Panne, R. Niessner, G. A. Petrucci, P. Cavalli, and N. Omenetto, "On-line and *in situ* detection of lead aerosols by plasma-spectroscopy and laser-excited atomic fluorescence spectroscopy," *Anal. Chim. Acta* **346**, 37–48 (1997).
9. J. P. Singh, F. Y. Yueh, H. S. Zhang, and R. L. Cook, "Study of laser induced breakdown spectroscopy as a process monitor and control tool for hazardous waste remediation," *Process Control Qual.* **10**, 247–258 (1997).
10. R. E. Neuhauser, U. Panne, R. Niessner, and P. Wilbring, "On-line monitoring of chromium aerosols in industrial exhaust streams by laser-induced plasma spectroscopy (LIPS)," *Fresenius J. Anal. Chem.* **364**, 720–726 (1999).
11. J. E. Carranza, B. T. Fisher, G. D. Yoder, and D. W. Hahn, "On-line analysis of ambient air aerosols using laser-induced breakdown spectroscopy," *Spectrochim. Acta Part B* **56**, 851–864 (2001).
12. D. W. Hahn, and M. M. Lunden, "Detection and analysis of aerosol particles by laser-induced breakdown spectroscopy," *Aerosol Sci. Technol.* **33**, 30–48 (2000).
13. D. W. Hahn, W. L. Flower, and K. R. Hencken, "Discrete particle detection and metal emissions monitoring using laser-induced breakdown spectroscopy," *Appl. Spectrosc.* **51**, 1836–1845 (1997).
14. D. W. Hahn, J. E. Carranza, G. R. Arsenault, H. A. Johnsen, and K. R. Hencken, "Aerosol generation system for development and calibration of laser-induced breakdown spectroscopy instrumentation," *Rev. Sci. Instrum.* **72**, 3706–3713 (2001).
15. J. E. Carranza, and D. W. Hahn, "Plasma volume considerations for analysis of gaseous and aerosol samples using laser-induced breakdown spectroscopy," *J. Anal. At. Spectrosc.* **74**, 5450–5454 (2002).
16. J. E. Carranza, and D. W. Hahn, "Assessment of the upper particle size limit for quantitative analysis of aerosols using laser-induced breakdown spectroscopy," *Anal. Chem.* **74**, 5450–5454 (2002).